On the Luminescence of $(Ba_{0.5}Sr_{0.5})_2SiO_4:Eu^{3+}$ upon X-ray Exposure

Max-Fabian Volhard and Thomas Jüstel
Department of Chemical Engineering, Münster University of Applied Sciences,
Stegerwaldstrasse 39, D-48565 Steinfurt, Germany

Keywords: Solid State Actinometer, $(Ba_{1-x/2}Sr_{1-x/2})_2SiO_4:Eu_x$, Ortho-Silicates, X-ray Excitation, X-ray Luminescence.

Abstract: Eu^{2+} doped ortho-silicates are widely applied as luminescent materials in phosphor converted light emitting diodes (pcLEDs) (Park et al. 2003; Jüstel et al. 2012), due to their high quantum yield, strong absorption, short decay time, and long-term stability upon blue light excitation.
The optical properties of $(Ba_{1-x/2}Sr_{1-x/2})_2SiO_4:Eu_x$ upon x-ray radiation are, however, much less known and were thus analysed in this work. It turned out that the activator ions in Eu^{3+} activated ortho-silicates are reduced to Eu^{2+} upon excitation by high energy radiation (> 5.0 eV). This reduction process can be monitored by the fading of the red line emission of Eu^{3+} in the range between 590 and 710 nm, originating from the $[Xe]4f^6$-$[Xe]4f^6$ transitions of Eu^{3+}. At the same time, a novel green broad emission band caused by the interconfigurational transition $[Xe]4f^7$-$[Xe]4f^65d^1$ shows up (fig. 1). This spectral change is a function of the irradiation period and can be quantified by the colour point shift of the emitted spectrum as well (fig. 2).

1 INTRODUCTION

Luminescent materials for the detection of high energy radiation are widely applied as storage materials. These storage phosphors consist of a host material comprising defects. Such defects are e.g. hole traps located above the valence band or electron traps below the conduction band. The storage material is charged by high energy radiation, which promote charge carriers from the valence band to the conduction band. There are two mechanisms to release the charge carriers. In the first case the traps are not deep enough and the charge carriers have the chance to leave the traps at room temperature. This process is known as afterglow or persistent luminescence. If the traps are deep enough, much deeper than the energy related to ambient temperature, there is no way for the charge carriers to leave the traps without stimulation via lattice vibration or optical photons (Kulesza et al. 2015; Blasse & Grabmaier 1994).
Storage phosphors such as $BaFBr:Eu^{2+}$ or $BaFCl:Eu^{2+}$ (Li et al. 2002; Secu et al. 2000) are common for this application area. In order to analyse the radiation dose of a storage phosphor, the functional principle via stimulation of the traps is complicated with a rather high relative uncertainty (Kulesza et al. 2015; Blasse & Grabmaier 1994).

This work describes the detection of high energy radiation via the change of photoluminescence properties. It turned out that the activator ions in Eu^{3+} activated ortho-silicates are reduced to Eu^{2+} upon excitation by high energy radiation (> 5.0 eV). This reduction process can be monitored by the fading of the red line emission of Eu^{3+} in the range between 590 and 710 nm, originating from the $[Xe]4f^6$-$[Xe]4f^6$ transitions of Eu^{3+}. Other materials where the change of luminescence upon high energy radiation has already been described are Ga_2O_3 (from red to blue) and Sr_2SiO_4 (from orange-red to yellow-white) (Nag & Kutty 2004; Layek et al. 2015).
Therefore, these Eu^{3+} doped ortho-silicates are promising candidates for the application in a solid state actinometer, which can be used to monitor a perceived x-ray radiation dose. Another application field could be the 2D x-ray mapping in flat detectors, wherein each phosphor particle can be individually read out after the x-ray exposure.

2 EXPERIMENTAL

All samples were synthesized by a high temperature solid state reaction. $BaCO_3$ (Alfa Aesar, 99,8%), $SrCO_3$ (Aldrich, 99,9%), Eu_2O_3 (Treibacher,

Volhard M. and JÃijstel T.
On the Luminescence of (Ba0.5Sr0.5)2SiO4:Eu3+ upon X-ray Exposure.
DOI: 10.5220/0006269101220125
In *Proceedings of the 5th International Conference on Photonics, Optics and Laser Technology (PHOTOPTICS 2017)*, pages 122-125
ISBN: 978-989-758-223-3

99,99%) and SiO_2 (Merck) were used as starting materials without further purification. The educts were weighted in stoichiometric amounts, thoroughly blended as acetone slurry in an agate mortar. For the substitution of Eu^{3+} for Sr^{2+}/Ba^{2+} no charge compensation was performed. The suspension was dried at ambient temperatures and was then transferred into an alumina boat. The powder was calcined at 1350 °C for 4 h in an oxygen atmosphere (Westfalen AG). After firing the phosphor was cooled down and ground to a fine powder again.

The phase purity of the samples was validated by using x-ray powder diffraction (XRD). The XRD measurements were performed on a Rigaku Miniflex II (Cu Kα; 30 kV; 15 mA), operating between 10° and 80° (2θ) with a step width of 0,02° and an integration time of 5°/min.

Optical properties like PLE and PL were measured on an Edinburgh Instruments FLS 920, which is equipped with an Xe arc lamp (450 W) and a cooled single photon PMT detection unit (Hamamatsu R2658P). Diffuse reflectance spectra were measured using an Edinburgh Instruments FS 920 spectrometer. This device is equipped with Xe arc lamp, a cooled single photon PMT detection Hamamatsu R928 and a spectralon sphere coated with Teflon. It was measured against a white standard ($BaSO_4$, 99,998%).

X-ray exposure tests were measured using a Rigaku Miniflex II (Cu Kα; 30 kV; 15 mA; 450 W). The samples were transferred into sample carriers and irradiated for different time periods between 40° and 41° (2θ).

3 RESULTS AND DISCUSSION

The phase purity of $(Ba_{0.5}Sr_{0.5})_2SiO_4:Eu^{3+}$ was proven by XRD. The herein investigated ortho-silicates crystallise in an orthorhombic crystal structure with a space group *Pnma* (#62) wherein two different Ba^{2+}/Sr^{2+} sites exist (Wang et al. 2013). Eu^{3+} (0,112 nm CN = 9) is a somewhat smaller than Ba^{2+}/Sr^{2+} (Ba^{2+}: 0,147 nm; Sr^{2+}: 0,131 nm; CN = 9) and occurs on the Ba^{2+}-sites (Ahrens 1952). Figure 1 shows the XRD pattern of $(Ba_{0.5}Sr_{0.5})_2SiO_4:Eu^{3+}$ and the respective ICDD reference card of the orthorhombic Ba_2SiO_4. The comparison confirms that there is no phase impurity present.

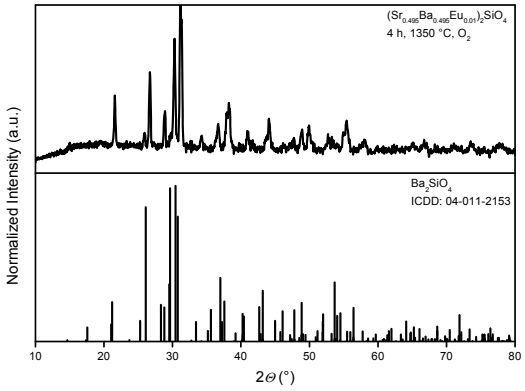

Figure 1: XRD pattern of $(Ba_{0.5}Sr_{0.5})_2SiO_4:Eu^{3+}$ and ICDD reference card 04-011-2153 of Ba_2SiO_4.

Optical properties of chemically reduced $(Ba_{0.5}Sr_{0.5})_2SiO_4:Eu^{2+}$ were investigated by measuring the PLE, PL and reflectance spectra (Figure 2). The excitation spectrum was monitored at λ_{em} = 612 nm and it is shown a broad excitation band between approx. 250 nm to 500 nm with a maximum at about 427 nm caused by $[Xe]4f^7$-$[Xe]4f^65d^1$ transition. A green broad emission band between 470 nm to 650 nm with a maximum at about 524 nm was observed monitoring at 427 nm. $(Ba_{0.5}Sr_{0.5})_2SiO_4:Eu^{3+}$ shows a high reflectance among 500 – 800 nm and a strong absorption band below 500 nm resulted by $[Xe]4f^7$-$[Xe]4f^65d^1$ transition.

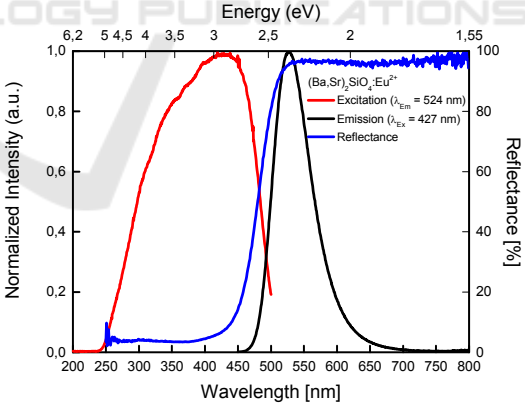

Figure 2: Room temperature PLE, PL and Reflectance spectra of $(Ba_{0.5}Sr_{0.5})_2SiO_4:Eu^{2+}$.

Figure 3 depicts the photoluminescence and the reflectance of a typical $(Ba_{0.5}Sr_{0.5})_2SiO_4:Eu^{3+}$ sample. The excitation spectrum was monitored at λ_{em} = 612 nm. Many parity forbidden $[Xe]4f^6$-$[Xe]4f^6$ transitions are observed, as it is typical for trivalent Europium. The $^7F_0$ ➔ $^5L_7$ (394 nm) transition shows the highest absorption strength. PL

of the Eu^{3+} phosphor was recorded for excitation at 394 nm. There are a set of emission lines corresponding to the intraconfigurational $^5D_0$ ➔ ^7F_J (J = 0-5) transitions. In the visible region the reflectance is nearly 100% and decrease below 350 nm due to $^7F_0$ ➔ $^5H_6$ transition (Baur & Jüstel 2015; QIAO et al. 2009).

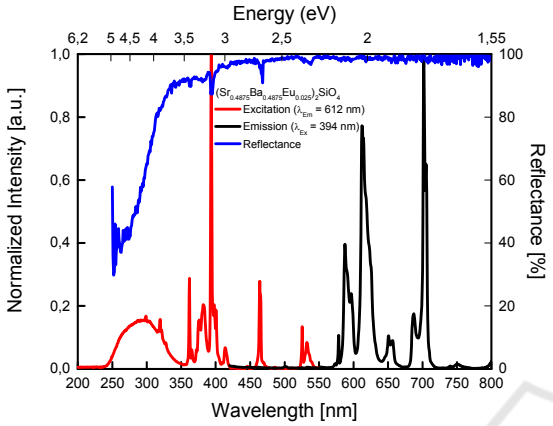

Figure 3: Room temperature emission, excitation, and reflection spectra of $(Ba_{0.5}Sr_{0.5})_2SiO_4:Eu^{3+}$.

It was observed that the described ortho-silicate reacts with high energy radiation (> 5.0 eV) and the activator cation was reduced from Eu^{3+} to Eu^{2+}. Figure 4 illustrate the emission spectra monitored at λ_{ex} = 394 nm in respect of x-ray exposure time. Without x-ray radiation there is only the Eu^{3+} lines emission observed. The exposure time was increased in 30 s steps and measured the PL properties. It was shown that the line emission of Eu^{3+} decreases with exposure time and the green broad band emission (Eu^{2+}) was increased. In temperature phosphor thermometry it is well proved that the temperature is measured via the ratio of two emission lines/bands. This method should also be possible for the measurement of the radiation dose (Hertle et al. 2017; Rabasović et al. 2016). Figure 5 shows $(Ba_{0.5}Sr_{0.5})_2SiO_4:Eu^{3+}$ after x-ray exposure. It was used an ortho-silicate without any stabilisation (e.g. Li^+ or Na^+), because a stabilised Eu^{3+} avoid reduction. There is a possibility for a back reaction to Eu^{3+}. At 500 °C (or higher) for 4 h in air, it was measured that all Eu^{2+} particles were oxidized.

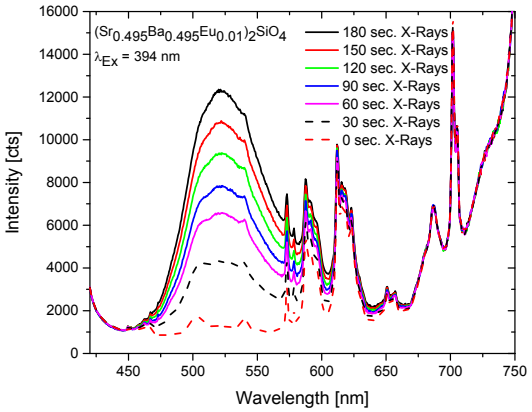

Figure 4: Emission spectra of $(Ba_{0.5}Sr_{0.5})_2SiO_4:Eu^{3+}$ upon 394 nm excitation after exposure to x-ray radiation as function of the exposure period.

Figure 5: Luminescence of $(Ba_{0.5}Sr_{0.5})_2SiO_4:Eu^{3+}$ (red emission) and $(Ba_{0.5}Sr_{0.5})_2SiO_4:Eu^{2+}$ (green emission) after x-ray exposure.

The perceived emission colour is a result of additive colour mixing of the line emission of remaining Eu^{3+} particles and of the broad band emission of Eu^{2+}-particles. The CIE 1931 colour diagram depicts the colour points of a $(Ba_{0.5}Sr_{0.5})_2SiO_4:Eu^{3+}$ sample treated for different exposure times. It nicely shows the colour change (Figure 6 and Table 1).

Table 1: Calculated colour points of $(Ba_{0.5}Sr_{0.5})_2SiO_4:Eu^{3+}$ upon 394 nm excitation after exposure to x-ray radiation as function of the exposure period.

Time [s]	x	y
0	0.4699	0.3923
30	0.3984	0.4676
60	0.3702	0.4974
90	0.3611	0.5088
120	0.3496	0.5203
150	0.3422	0.5285
180	0.335	0.5357

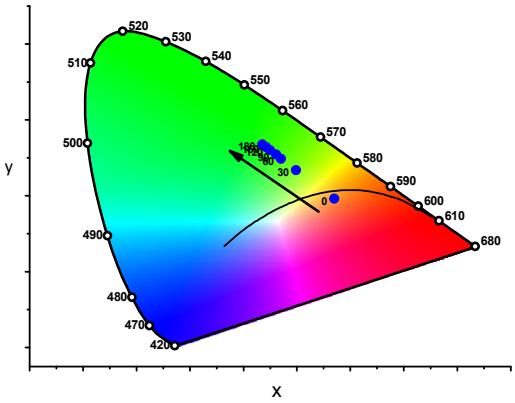

Figure 6: CIE1931 colour triangle comprising the colour points x, y of a $(Ba_{0.5}Sr_{0.5})_2SiO_4:Eu^{3+}$ sample upon 394 nm excitation after exposure to x-ray radiation as function of the exposure period.

4 CONCLUSIONS

A solid state reaction was used to prepare $(Ba_{0.5}Sr_{0.5})_2SiO_4:Eu^{3+}$ without applying co-dopants for valence state stabilisation. This phosphor exhibits strong 4f-4f line emission at around 590, 613, and 705 nm. Upon x-ray exposure, the photoluminescence changes to a green broad band emission, which can be assigned to the formation of divalent Europium. First results show that a strong dependence between exposure time and the intensity of Eu^{2+} emission exists.

Therefore, these Eu^{3+} doped ortho-silicates are promising candidates for the application in a solid state actinometer, which can be used to monitor a perceived x-ray radiation dose. Another application field could be the 2D x-ray mapping in flat detectors, wherein each phosphor particle can be individually read out after the x-ray exposure. The detectors can be easily reactivated, since it was shown that the process was completely reversible at a temperature of about 500 °C.

ACKNOWLEDGEMENTS

The authors are grateful to Merck KGaA Darmstadt, Germany for their generous financial support.

REFERENCES

Ahrens, L.H., 1952. The use of ionization potentials Part 1. Ionic radii of the elements. *Geochimica et Cosmochimica Acta*, 2(3), pp.155–169.

Baur, F. & Jüstel, T., 2015. New red-emitting phosphor La2Zr3(MoO4)9:Eu3+ and the influence of host absorption on its luminescence efficiency. *Australian Journal of Chemistry*, 68(11), pp.1727–1734.

Blasse, G. & Grabmaier, B.C., 1994. *Luminescent materials*, Berlin: Springer.

Hertle, E. et al., 2017. Influence of codoping on the luminescence properties of YAG:Dy for high temperature phosphor thermometry. *Journal of Luminescence*, 182, pp.200–207. Available at: http://linkinghub.elsevier.com/retrieve/pii/S0022231316310602.

Jüstel, T. et al., 2012. Luminescent Materials. In *Ullmann's Encyclopedia of Industrial Chemistry*. Wiley-VCH, p. Vol. A1-28.

Kulesza, D. et al., 2015. Lu2O3-based storage phosphors. An (in)harmonious family. *Coordination Chemistry Reviews*, 325, pp.29–40. Available at: http://dx.doi.org/10.1016/j.ccr.2016.05.006.

Layek, A. et al., 2015. Dual Europium Luminescence Centers in Colloidal Ga2O3 Nanocrystals: Controlled in Situ Reduction of Eu(III) and Stabilization of Eu(II). *Chemistry of Materials*, 27(17), pp.6030–6037.

Li, H. et al., 2002. Imaging performance of polycrystalline BaFBr:Eu2+ storage phosphor plates. *Materials Science and Engineering*, 94, pp.32–39.

Nag, A. & Kutty, T.R.N., 2004. The light induced valence change of europium in Sr2SiO4 : Eu involving transient crystal structure. *Journal of Materials Chemistry*, 14, pp.1598–1604.

Park, J.K. et al., 2003. White light-emitting diodes of GaN-based Sr2SiO4:Eu and the luminescent properties. *Applied Physics Letters*, 82(5), pp.683–685.

QIAO, Y. et al., 2009. Photoluminescent properties of Sr2SiO4:Eu3+ and Sr2SiO4:Eu2+ phosphors prepared by solid-state reaction method. *Journal of Rare Earths*, 27(2), pp.323–326. Available at: http://dx.doi.org/10.1016/S1002-0721(08)60243-4.

Rabasović, M.D. et al., 2016. Luminescence thermometry via the two-dopant intensity ratio of $Y_2O_3:Er^{3+}$, Eu^{3+}. *Journal of Physics D: Applied Physics*, 49(48), p.485104. Available at: http://stacks.iop.org/0022-3727/49/i=48/a=485104?key=crossref.3200e650b81c0991bac2b761c8aa7d84.

Secu, M. et al., 2000. Preparation and optical properties of BaFCl:Eu2+ X-ray storage Phosphor. *Optical Materials*, 15, pp.115–122.

Wang, Z. et al., 2013. Luminescent properties of Ba2SiO4:Eu3+ for white light emitting diodes. *Physica B: Condensed Matter*, 411, pp.110–113. Available at: http://dx.doi.org/10.1016/j.physb.2012.11.040.